Earth-Science Reviews 107 (2011) 66–75

Contents lists available at ScienceDirect

Earth-Science Reviews

journal homepage: www.elsevier.com/locate/earscirev

Insights on the 2009 South Pacific tsunami in Samoa and Tonga from field surveys and numerical simulations

Hermann M. Fritz [a,*], Jose C. Borrero [b,c], Costas E. Synolakis [c,d], Emile A. Okal [e], Robert Weiss [f], Vasily V. Titov [g], Bruce E. Jaffe [h], Spyros Foteinis [d], Patrick J. Lynett [i], I.-Chi Chan [j], Philip L.-F. Liu [j]

[a] School of Civil and Environmental Engineering, Georgia Institute of Technology, Savannah, GA 31407, USA
[b] ASR Limited, Raglan 3225, New Zealand
[c] Department of Civil and Environmental Engineering, Univ. of Southern California, Los Angeles, CA, USA
[d] Department of Environmental Engineering, Technical University of Crete, Chanea 73100, Greece
[e] Department of Earth and Planetary Sciences, Northwestern University, Evanston, IL, USA
[f] Department of Geology and Geophysics, Texas A&M University, College Station, TX, USA
[g] Pacific Marine Environmental Laboratory, NOAA, Seattle, WA, USA
[h] Pacific Science Center, US Geological Survey, Santa Cruz, CA, USA
[i] Department of Civil Engineering, Texas A&M University, College Station, TX, USA
[j] School of Civil and Environmental Engineering, Cornell University, Ithaca, NY, USA

ARTICLE INFO

Article history:
Received 16 July 2010
Accepted 3 March 2011
Available online 10 March 2011

Keywords:
tsunami
earthquake
South Pacific
Samoa
Tonga

ABSTRACT

An $M_w \approx 8.1$ earthquake south of the Samoan Islands on 29 September 2009 generated a tsunami that killed 189 people. From 4 to 11 October, an International Tsunami Survey Team surveyed the seven major islands of the Samoan archipelago. The team measured locally focused runup heights of 17 m at Poloa and inundation of more than 500 m at Pago Pago. A follow-up expedition from 23 to 28 November surveying the three main islands of Tonga's northernmost Niua group revealed surprising 22 m runup and 1 km inundation. We analyze the extreme tsunami runup and complex impact distribution based on physical and societal observations combined with numerical modeling. That an outer rise/outer trench slope (OR/OTS) event is responsible for a tsunami disaster in the Pacific calls for care in identifying and defining tsunami hazards. Evacuation exercises conducted in Samoa in the preceding year may have limited the human toll; however, cars were identified as potential death traps during tsunami evacuations. This event highlights the extreme hazards from near source tsunamis when the earthquake's shaking constitutes the de facto warning, and further underscores the importance of community based education and awareness programs as essential in saving lives.

© 2011 Elsevier B.V. All rights reserved.

Contents

* Corresponding author. Tel.: +1 912 966 7947.
E-mail address: fritz@gatech.edu (H.M. Fritz).

0012-8252/$ – see front matter © 2011 Elsevier B.V. All rights reserved.
doi:10.1016/j.earscirev.2011.03.004

1. Event overview

On September 29, 2009 at 17:48:10 UTC (6:48:10 local time), an $M_w \approx 8.1$ earthquake struck ~200 km S of the main Samoan Islands chain and ~75 km E of Tonga's Niua Group. This is the most significant earthquake on the northern bend of the Tonga trench since 1917 (Okal et al., 2004). This event does not represent simple subduction of the Pacific plate into the Tonga trench, but rather started as a normal faulting rupture expressing a lateral tear in the plate as it slides past the Northern bend of the plate boundary (Okal et al., 2010). It then triggered a smaller, but still substantial episode of interplate thrusting, as modeled by Li et al., 2009 and later Lay et al., 2010. Such events are known elsewhere (Govers and Wortel, 2005), but their recurrence is, if anything, even more poorly understood than for great subduction earthquakes; five large OR/OTS events versus 59 mega-thrusts have been identified since 1900 (Kirby et al., 2009). That another non-subduction source mechanism is responsible for yet another tsunami disaster in the South Pacific is a call for care in identifying and defining tsunami hazards.

The ensuing tsunami killed 9 in Tonga, 146 in Samoa, and 34 in American Samoa, the highest tsunami death toll on US territory since 1964. The damage in Samoa alone exceeded $150 million (UN-OCHA). A tsunami warning issued 16 min after the earthquake was too late for many, as the tsunami arrived within 15 min at some of the hardest hit villages. Fortunately, many Samoans and Tongans knew to get to high ground after experiencing an earthquake, a behavior enhanced by education and evacuation exercises initiated throughout the South Pacific over the past decade; in Samoa, the latter had taken place in the preceding year.

2. Post-tsunami reconnaissance

The surveys we report took place from 4 to 11 October covering the entire Samoan archipelago, including the islands of Upolu, Savai'i, Manono, Tutuila, Aunu'u, Ofu and Olosega, and from 23 to 28 November focusing on the Niua group (Niuatoputapu, Tafahi and Niuafo'ou islands) of the Tongan archipelago. The survey teams documented tsunami runup, flow depth and inundation; wave induced deposition or erosion, structural damage and interviewed eyewitnesses according to protocols reviewed by Synolakis and Okal (2005). The recorded combined Samoa and Tonga survey database is composed of 444 tsunami runup and flow depth measurements (Okal et al., 2010). Eyewitnesses described between one and four main waves with an initial recession, interpreted as a leading depression N-wave (Tadepalli and Synolakis, 1994). Several eyewitnesses reported evacuating only after watching others do so or upon observing the first wave. Most drivers did not feel the earthquake inside their cars. There were also cases of victims killed in cars, overcome by the wave while stopped in traffic during the evacuation. This was an unfortunate occurrence possibly attributable to confusion resulting from conflicting official statements recently issued in Samoa on the use of vehicles during a tsunami evacuation. Indeed, part of the rationale for Samoa changing from left to right hand drive on 7 September 2009, just 3 weeks before the tsunami, was justified as a step to reduce greenhouse gases, through the availability of used cars from Australia and New Zealand, and to allow more citizens to own cars and thus escape from the sea shore (WSJ, 2009). Similarly, seven of the victims on Niuatoputapu were riding a truck that was subsequently caught by the tsunami while heading back to the high-school to pick-up the principal who had, in the meantime, already evacuated. An additional Tongan victim at Hihifo returned to his house to close a shop between tsunami waves. Only the keeper of the Palm Tree Island Resort located across the tidal channel from Hihifo on Hunganga Island, which was totally submerged by tsunami waves, was an unpreventable fatality in the Kingdom of Tonga.

3. Observations in the Samoan archipelago

Fig. 1 shows the measured flow depths and runup heights throughout the Samoan archipelago. The data exhibit pronounced extrema and significant variation on all main islands. On Tutuila, a maximum runup spike exceeded 17 m at Poloa, near the western tip, where damage was extensive and reminiscent of the impact of the 2004 tsunami in many locales in Sri Lanka (Liu et al., 2005). The tsunami wrackline and rafted debris at Poloa along a relatively steep transect with a short 100 m distance from shoreline to maximum runup are shown Fig. 2c–e. Runup decreased somewhat along Tutuila from west to east reaching 12 m at Fagasa, on the central north coast and 9 m at Tula in the east. Pago Pago,

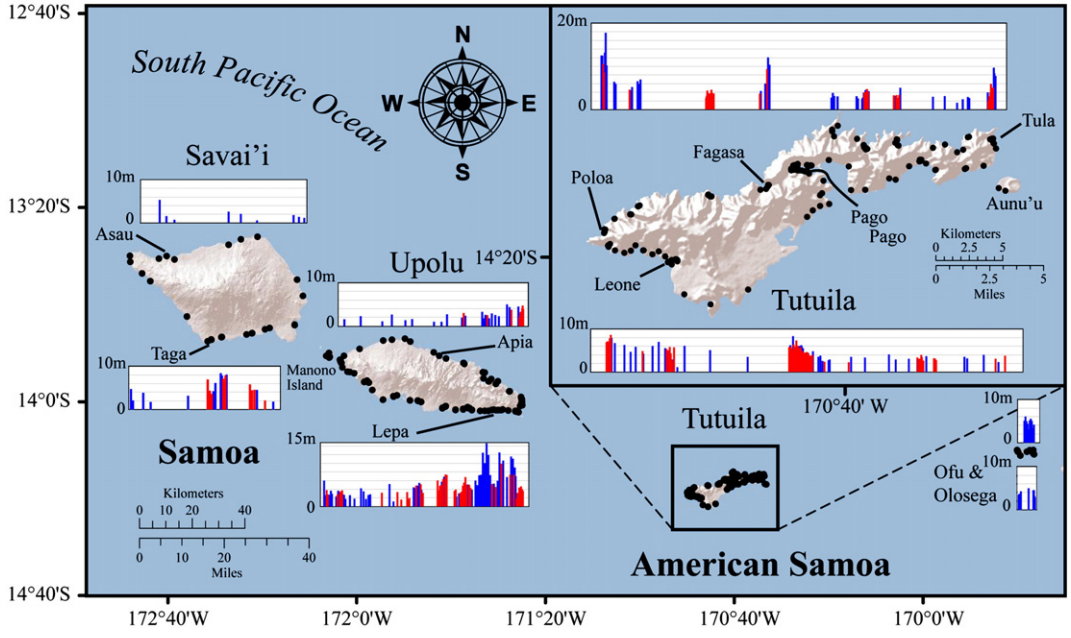

Fig. 1. Samoan Islands with measured tsunami runup (blue) and tsunami height $z + h$ (red) at survey locations on south and north coasts. Runup and tsunami height $z + h$ are relative to the sea level at time of tsunami arrival with z terrain elevation and h flow depth above terrain.

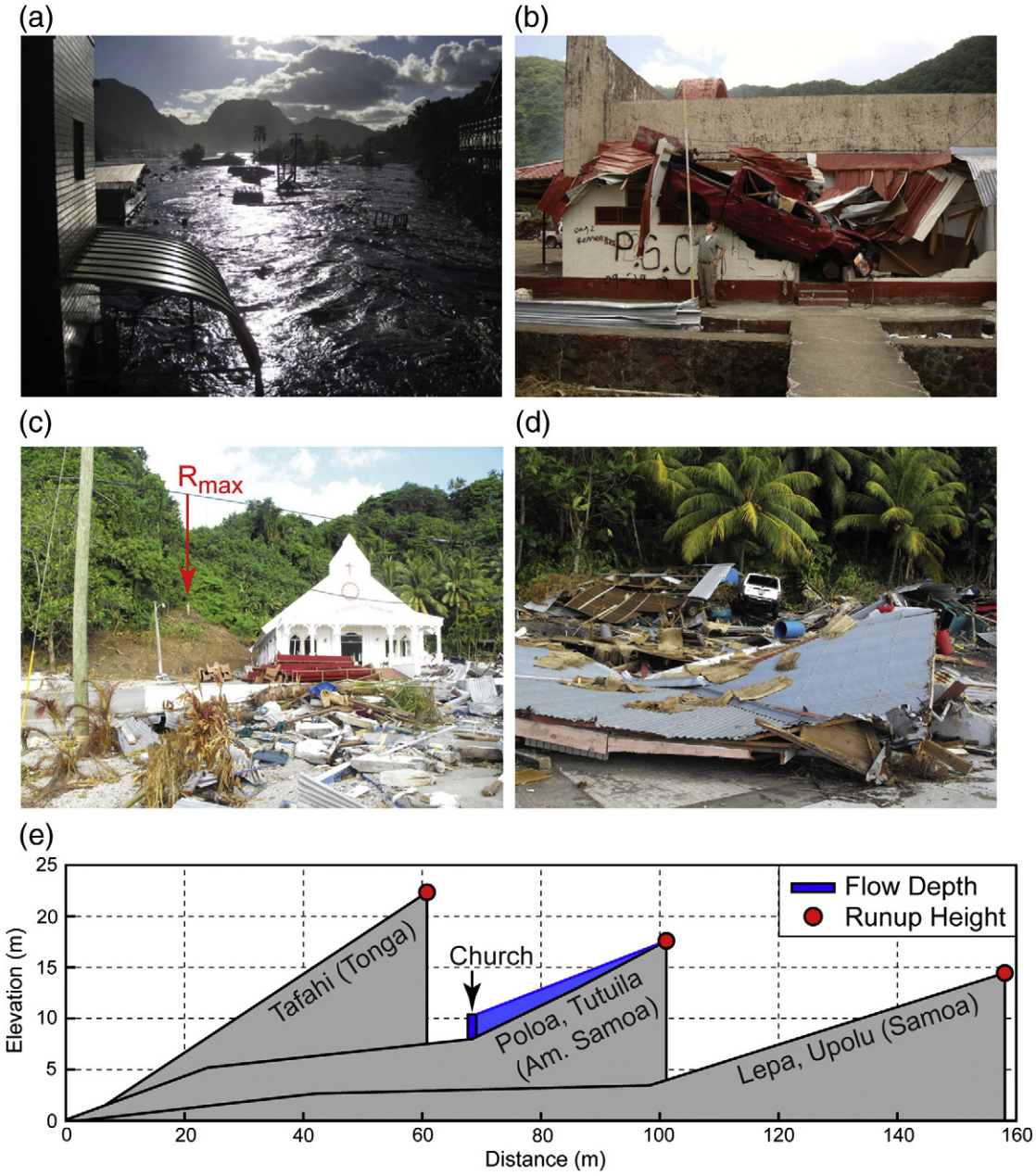

Fig. 2. Tutuila, American Samoa field observations: (a) Pago Pago: First wave receding with a water level ~1 m below maximum flood levels in a morning eastward view 250 m from the shoreline at location PA in Fig. 3 (photo: Gordon Yamazaki, NOAA); (b) Pago Pago: Vehicle projectile impact 300 m from the shoreline and flow depth measurement at location PB in Fig. 3; (c) Poloa: Trimline in vegetation behind the church marks the maximum runup of 17 m; (d) Poloa: Multiple vehicles piled up within tsunami debris deposit; (e) comparison of surveyed transects from the beach to the maximum runup height at Tafahi (Tonga), Poloa (American Samoa) and Lepa (Upolu, Samoa).

central south coast, represents an unfortunate example of a town and harbor whose geometry is ideal for protection against storm waves but leaves it vulnerable to tsunami inundation, similar to villages on Babi Island near Flores, Indonesia (Yeh et al., 1994) and Rendova Harbor in the Solomon Islands (Fritz and Kalligeris, 2008). The harbor geometry at Pago Pago (Fig. 3) amplified the tsunami from just a few meters at the entrance to 8 m at the head, causing extensive flooding and structural damage over 500 m inland up the Vaipito River. Several large boats and tens of vehicles were swept inland (Fig. 2). Overland flow speeds of the tsunami front were estimated from security camera footage to 2.5 m/s about 200 m onshore. This is similar to the initial-front speeds measured from amateur videos near the Grand Mosque in Banda Aceh during the 2004 tsunami, about 3 km inland (Fritz et al., 2006). One eyewitness described the flooding at Pago Pago as much more violent than during the 1960 Chilean tsunami, which had arrived in the evening.

In contrast to Tutuila, which had significant tsunami impact on both north and south coasts, destruction on the islands of Samoa was confined to the southern coasts. Coral reefs in Tutuila and Upolu did not substantially reduce the advancing tsunami where located in close proximity to the shoreline. A photograph of the advancing tsunami bore shoreward of the reef located 3 km offshore at Le Vasa in NW Upolu is shown in Fig. 4a. On Upolu, runup reached 14 m at Lepa (Fig. 4b). The transect at Lepa with a 160 m distance from shoreline to maximum runup is longer and less steep than at Poloa (Fig. 2e). In Lalomanu on the SE, the damage was quite reminiscent of Hambantota, Sri Lanka in 2004 (Liu et al., 2005), with only concrete slabs of structures left standing and extensive debris fields. The inundation distances on Upolu only exceeded 500 m inland along the Salani River, while in Sri Lanka the 2004 tsunami penetrated 2 to 3 km inland at several locations. Relatives of victims described how family members

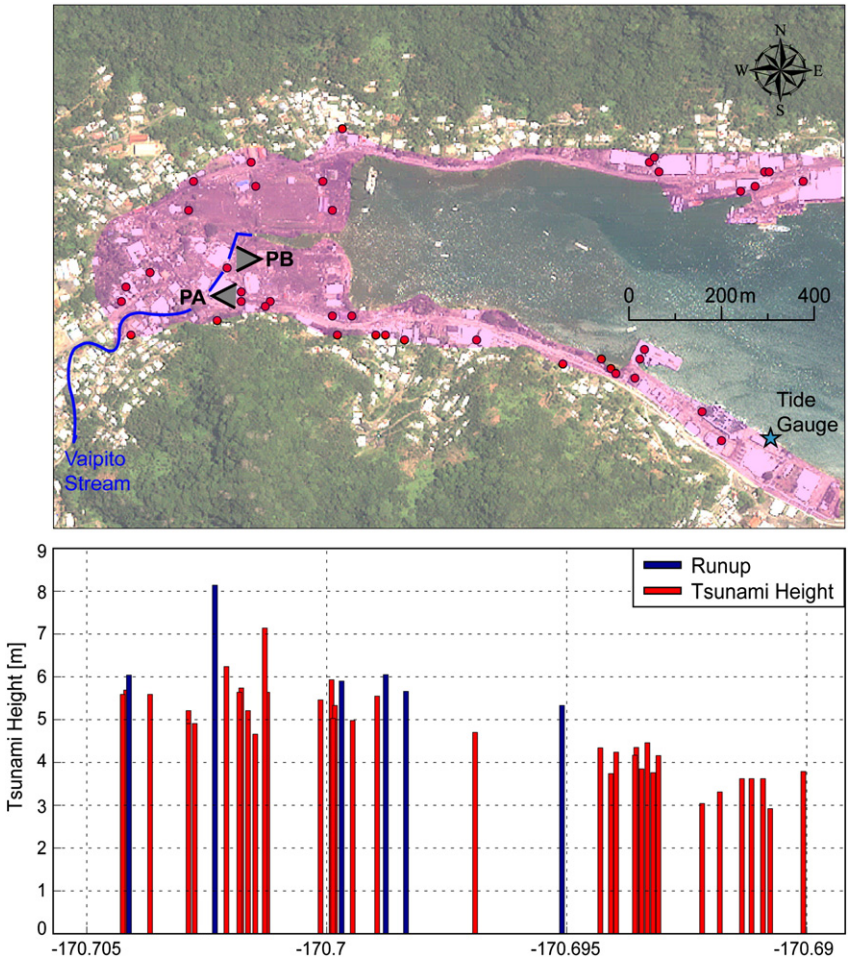

Fig. 3. Pago Pago, American Samoa in post-tsunami Quickbird satellite imagery with measured tsunami heights at survey locations inside the harbor and town with the locations of the tide gauge and photos PA and PB in Fig. 2. Runup and tsunami height $z+h$ are relative to the sea level at time of tsunami arrival with z terrain elevation and h flow depth above terrain.

had been trapped in their cars while trying to evacuate. On Savai'i, maximum runup exceeded 8 m at Nuu. At nearby Taga, a 6 m runup and ~200 m inundation left behind a boulder deposit field extending up to 100 m inland (Fig. 4c). The tsunami deposit's grain diameters range from medium cobble to boulder size. No obvious sorting could be observed from the shoreline toward the maximum runup. Cobbles and boulders are made up of chunks from the nearby lava flow. The porosity varies greatly, resulting in very different bulk densities with estimates varying between 2.0 t/m^3 and 1.4 t/m^3 depending on porosity. Similar deposits remained on the same roadway along the beach after a smaller tsunami in 1981 (Solov'ev et al., 1986).

4. Observations in the Tongan archipelago

The tsunami impact on Tonga's Niua group (Fig. 5) surprisingly eclipsed the Samoan observations in all aspects with maximum runup of 22 m on both the east and west coasts of Tafahi Island as well as flow depth of 15 m and inundation of 1 km on Niuatoputapu Island's east coast, which was reminiscent of the impact of the 2006 Java tsunami on Nusa Kambangan Island (Fritz et al., 2007). Tafahi represents tsunami impact on a volcanic island characterized by steep hill slopes up to 1 V:3 H (V: vertical, H: horizontal) and fringing reefs within 100 m of the shoreline. The transect with the maximum runup for the entire event at Tafahi is significantly shorter and steeper than both transects at Poloa and Lepa (Fig. 2e). Niuatoputapu's flat coastal topography and near shore fringing reefs allowed for massive inland penetration of the tsunami waves along the south and east coasts (Fig. 6). While forests may provide some tsunami attenuation at flow depths below 5 m, the forests on the south coast were completely overwhelmed by local flow depths of up to 10 m above the ground surface (Fig. 7). Fortunately, the coral reefs and tidal flats extending between 1 and 2 km offshore along Niuatoputapu's north shore reduced the tsunami impact for the villages located there. Nevertheless, 89 out of the 225 houses on Niuatoputapu were totally destroyed and 56 were damaged. The Tongan Government estimates the total cost of damage to US $ 9.5 million.

5. Tsunami modeling

To simulate the regional tsunami we used the model MOST (Titov and Gonzalez, 1997). Simulations were carried out on two sets of numerical grids to investigate both the near and far-field aspects of the tsunami. For the far field investigations, MOST was run as a propagation model only. Modeling was carried out on a bathymetry grid derived from the GEBCO global bathymetry dataset with a spatial resolution of 2 arcmin. For modeling the detailed inundation on Tutuila, a series of nested grids were created from a 3-arcsec DEM of American Samoa (NOAA-NGDC). The resolution of the innermost grid for the simulations presented in this study was 6-arcsec or approximately 180 m.

5.1. Tsunami source models

Five different source models were used to initialize the tsunami model (Fig. 8). These included a source model based on the USGS finite fault model (Hayes, 2009) which was used in initial simulations presented in Okal et al. (2010) as well as in simulation of the Samoa

Fig. 4. Samoa field observations: (a) Upolu: Tsunami bore advancing past the reef at Le Vasa between Manono and Upolu Islands (photo: Brandon Burke); (b) Upolu: Trimline in forest and debris mark the maximum runup of 14 m at Lepa (transect shown in Fig. 3e); (c) Savai'i: Cobble and boulder deposit covers field at Taga with 6 m runup and ~200 m inundation.

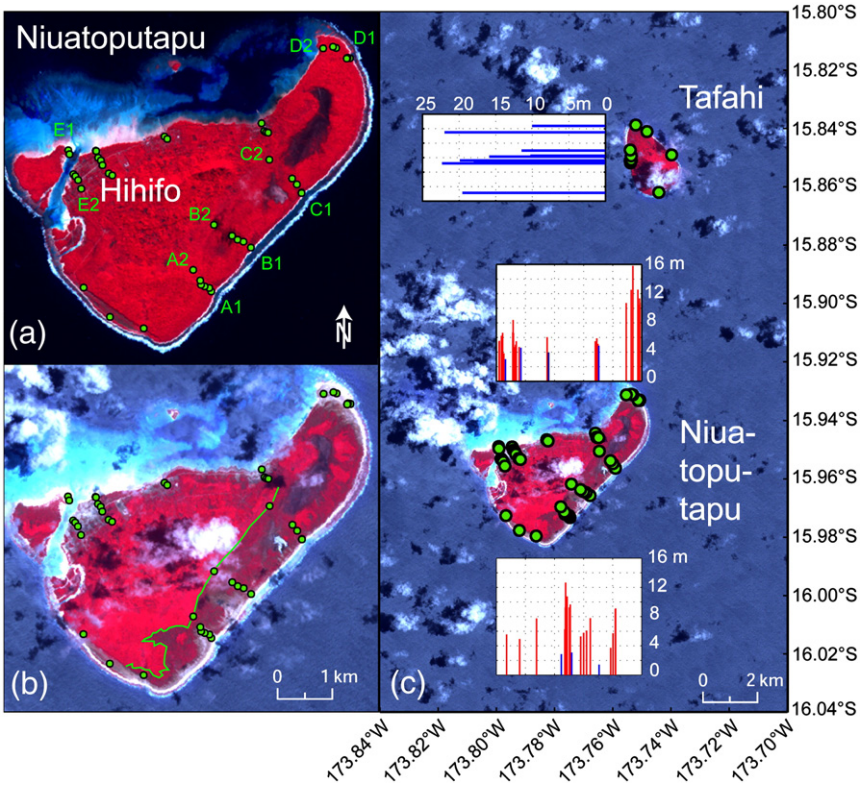

Fig. 5. Tonga's Niuatoputapu and Tafahi Islands in ASTER false-color satellite images acquired on: (a) July 25, 2006, (b and c) October 19, 2009 and (c) with measured tsunami runup (blue) and tsunami height $z+h$ (red). Image color code: (red) healthy vegetation, (dark red) salt-burned vegetation, (blue-gray) bare ground, (white, cyan) clouds and breaking waves. The elevation of the Sun in the sky was markedly different in those images resulting in ocean water appearing dark blue in the 2009 image and almost black in 2006 (satellite imagery courtesy: NASA).

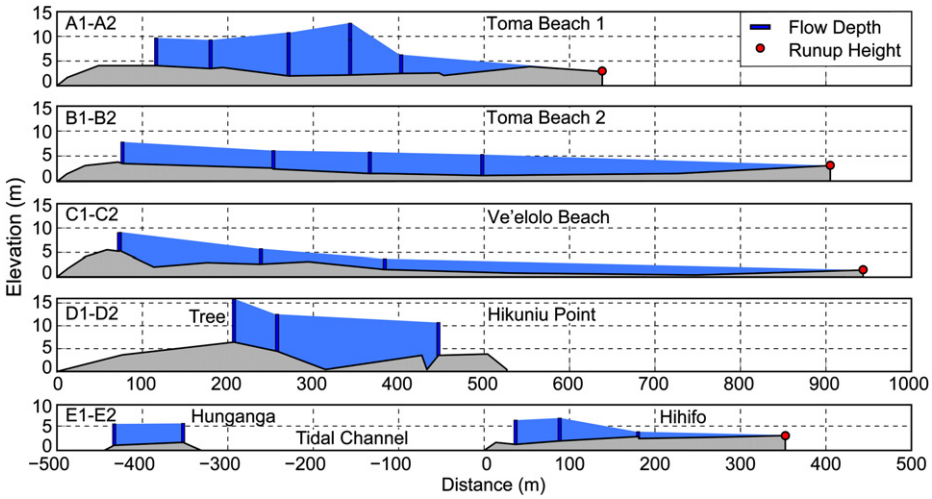

Fig. 6. Selected transects surveyed on Niuatoputapu and Hunganga Islands with the transect locations shown in Fig. 5.

tsunami presented in Roeber et al. (2010). Additionally, we explored the implications of using rectangular, single plane, uniform slip source models (Table 1). These included a single source, steeply dipping, outer-rise normal fault ('Normal 0') and a multi-source composite model. The composite fault model, comprised of an outer-rise normal fault in combination with a secondary thrust fault on the subduction zone interface is used by Beavan et al. (2010) in their geodetic modeling of this event. The normal fault and megathrust components of the composite source model are denoted 'Normal 1' and 'Mega 1' respectively. We use the same fault parameters (Table 1) suggested by Beavan et al. (2010) and compare the model results with the tidal record in Pago Pago Harbour and with the three nearest DART tsunameter stations.

We modeled the composite source in two ways; (1) by summing the deformation fields induced by each set of source parameters to make one deformation field and (2) by modeling each source separately, then adding a resultant time series extracted from the same location in each simulation to make a water level time history representative of a composite event. If the wave train can be described as linear throughout its evolution, the results from (1) and (2) above would be identical. This comparison will thus show the nonlinear effect, but will more importantly be used to present the individual wave trains from the Normal 1 and Mega 1 sources.

5.2. Model results: Tutuila

Preliminary efforts at modeling the Samoa tsunami, first reported in Okal et al. (2010), illustrated the insensitivity of the model results (and by proxy the tide gauge recordings), to the details of the seismic source,

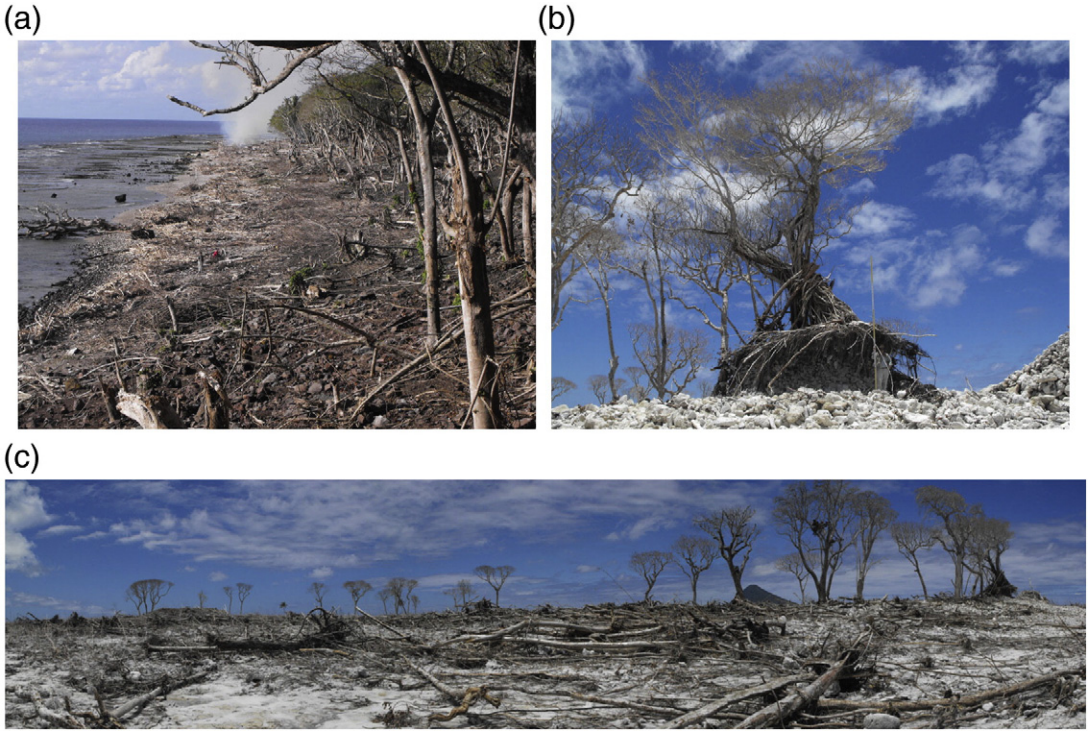

Fig. 7. Tonga field observations: (a) Tafahi Island in a N-view from the maximum 22 m runup with broken branches in the foreground and destroyed forest along the beach with team members (transect shown in Fig. 3e); Niuatoputapu Island's north tip: (b) broken branch and scars on the bark of a tree indicating 9.4 m flow depth above the ground surface at a site that was 6 m above sea level and 200 m from the beach (Hikuniu Point transect shown in Fig. 6). Note the scour of more than 2 m around the tree roots; (c) Forest overwhelmed by tsunami with felled and uprooted trees amidst coral boulders and cobbles.

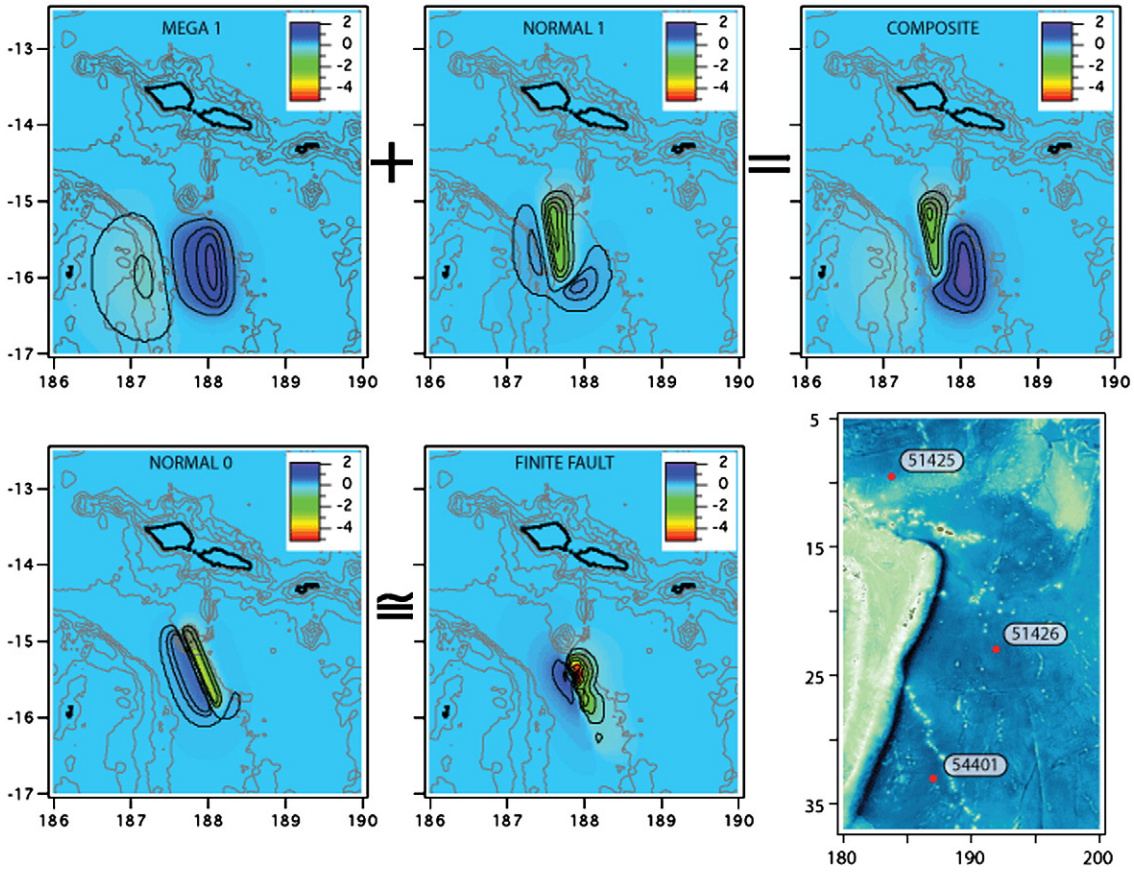

Fig. 8. The five earthquake deformation scenarios used to initialize the tsunami propagation model. (top row) Mega 1 and Normal 1, combined they make the composite source. (bottom row, left) the idealized normal fault scenario used by Beavan et al. (2010) meant to be a rough equivalent to the USGS finite fault model. (bottom row, middle) The USGS finite fault model used for initial tsunami modeling presented in Okal et al. (2010) and Roeber et al. (2010). (lower right) Propagation modeling domain with locations of the three nearest DART buoys.

with the same general findings replicated in this updated modeling effort. A comparison of the tide gauge recording from inside Pago Pago Harbor to the model simulations is shown in Fig. 9a–e. Panels a and b show the results from each component of the composite source. While the computed time series from the Normal 1 source match fairly well with the recorded data, there is a more significant difference between predicted and measured for the Mega 1 source (Fig. 9b). The time series for the component sources are compared in Fig. 9c, which shows that the two signals are nearly perfectly out of phase relative to each other. It is worth noting that a relative shift of 1 to 3 min of either time series, as suggested in recent investigations into the complex nature of the source (Beavan et al., 2010; Lay et al., 2010) would not bring the model results into phase with each other. Fig. 9d then combines the two events and compares the result to the measured data. It is clear from this figure that initializing the tsunami computation with a composite source (blue trace) does not produce a time series significantly different from the result obtained by summing the individual time series from the component sources (red trace). However, both results produce a fit to the measured data that is arguably worse than for the Normal 1 scenario on its own. Finally, the results from the Normal 0 and USGS finite fault sources are shown in Fig. 9e and f. Both of these sources produce a reasonably good fit to the measured data, particularly for the amplitude and duration of the first major fall, rise and fall of the water surface. However, the small rise in sea level prior to the sudden withdrawal is a vexing component of the measured time series that is not represented well in any of the simulations.

Table 1
Fault parameters for the single fault plane models used to initialize the tsunami propagation model.

	Normal 0	Normal 1	Mega 1
Length (km)	120	114	110
Width (km)	15	28	90
Dip (deg)	55	48	16
Rake (deg)	−60	−41	85
Strik (deg)	338	352	175
Slip (m)	9.9	8.6	4.1
Latitude (S)	15.940	15.34	15.542
Longitude (E)	187.282	187.96	187.763

In an attempt to improve the fit between the modeled and measured water levels at Pago Pago, we shifted the time series caused by the Mega 1 relative to the Normal 1 source. The time shifts covered the range in temporal offset between the two sources suggested by both Beavan et al. (2010) and Lay et al. (2010). In our convention, a positive shift puts the Mega 1 source prior to the Normal 1 source and vice versa. The results from these time shifts are shown in Fig. 10. While there is no clear improvement in the fit to the measured data for any of the shifts, the −0:27 and −0:54 shift cases (Fig. 10b, red and blue traces) show some promise, particularly with the presence of the small positive surge prior to the first large withdrawal.

5.3. Model results: Far field

The tsunami sources described above were also used to investigate the far-field signature of the tsunami as recorded on three DART tsunameters located in the southwestern Pacific Ocean (Fig. 8), at distances of 750 to 1900 km. Figs. 11 and 12 compare the modeled time series from the 5 sources to the DART data. Individually, the

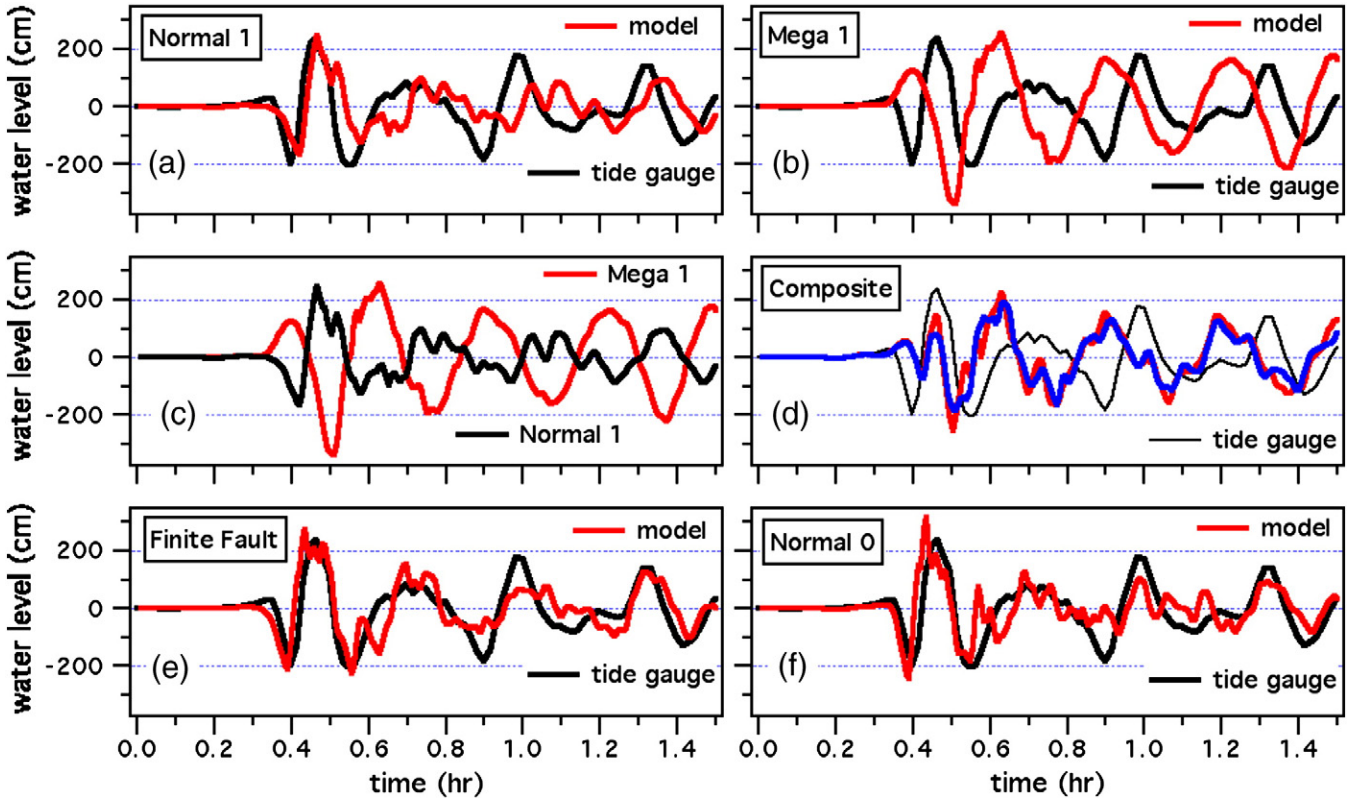

Fig. 9. Comparison between measured and modeled tsunami wave heights in Pago Pago Harbour. (a and b) Comparison between each component of the composite source proposed by Beavan et al. (2010) to the measured tide gauge record. (c) The two components time series on the same plot showing the relative contribution of each. (d) The red trace is the summation of the time series from each source while the blue trace is the time series extracted from a simulation using the composite source model. The thin black trace is the tide gauge data. (e and f) Time series from the USGS finite fault and the Normal 0 case compared to the tide gauge record.

Mega 1 source produces a very good fit to the measured data, particularly on gauges 51426 and 54401. The Normal 1 source does not fit as well overall, but does do a good job at reproducing the initial drawdown seen on DART 51425. The composite time series does not provide a clear improvement of the fit between the modeled and measured data. The Normal 0 and Finite Fault cases (Fig. 12) produce similarly bad results in comparison to the measured data. The modeled initial wave at station 51426 is overly steep and with a significantly larger negative amplitude while on stations 51426 and 54401, the modeled signal has an inverse

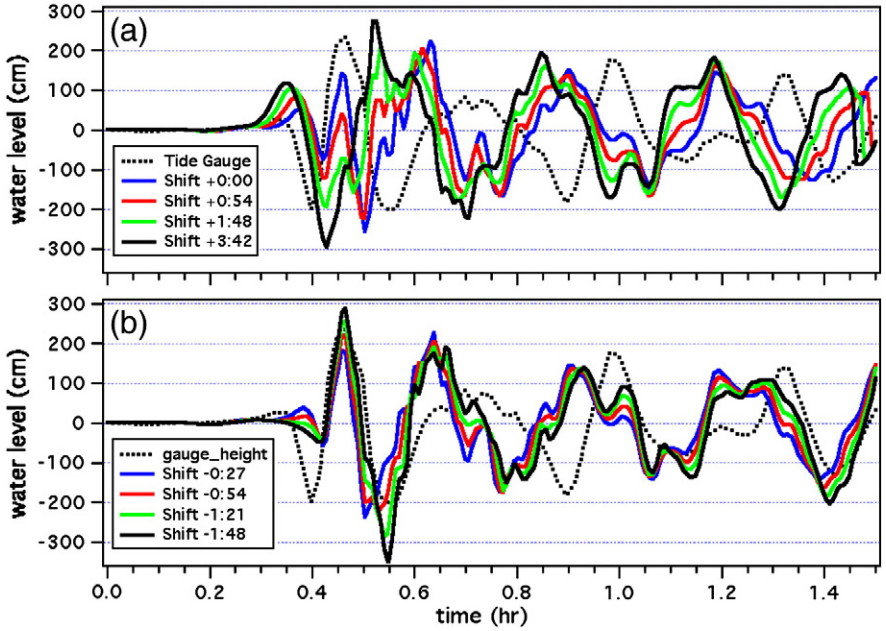

Fig. 10. The result of time-shifting the Mega 1 source time series relative to the Normal 1 time series. A positive shift means the Mega 1 source preceded the Normal 1 source. No significant improvement is obvious for the positive shift, whereas some improvement is evident with a small negative time shift.

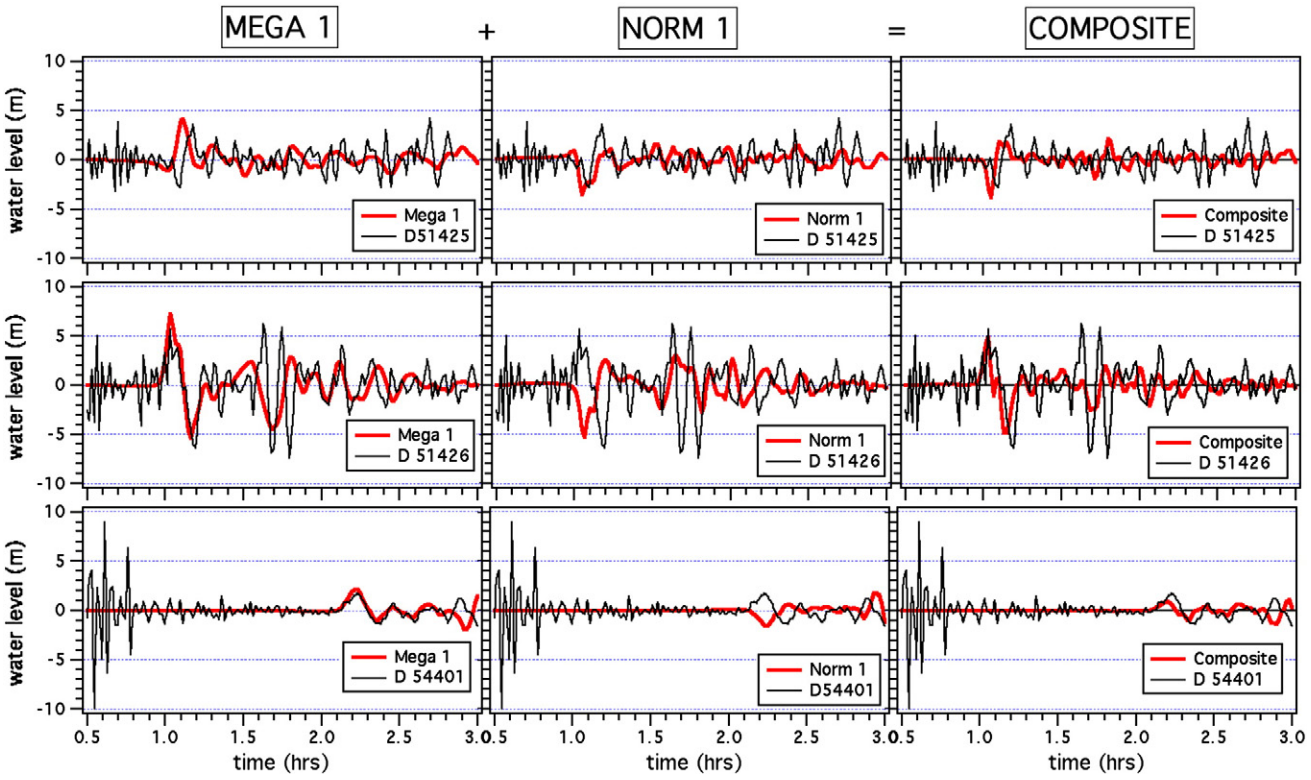

Fig. 11. Comparison between modeled (red) and measured water levels at three DART tsunameter locations. The contribution of the two components in the composite source can be seen. The time series generated by Mega 1 and Norm 1 are summed to produce the composite time series. An improvement to the fit between the modeled and measured data can be seen.

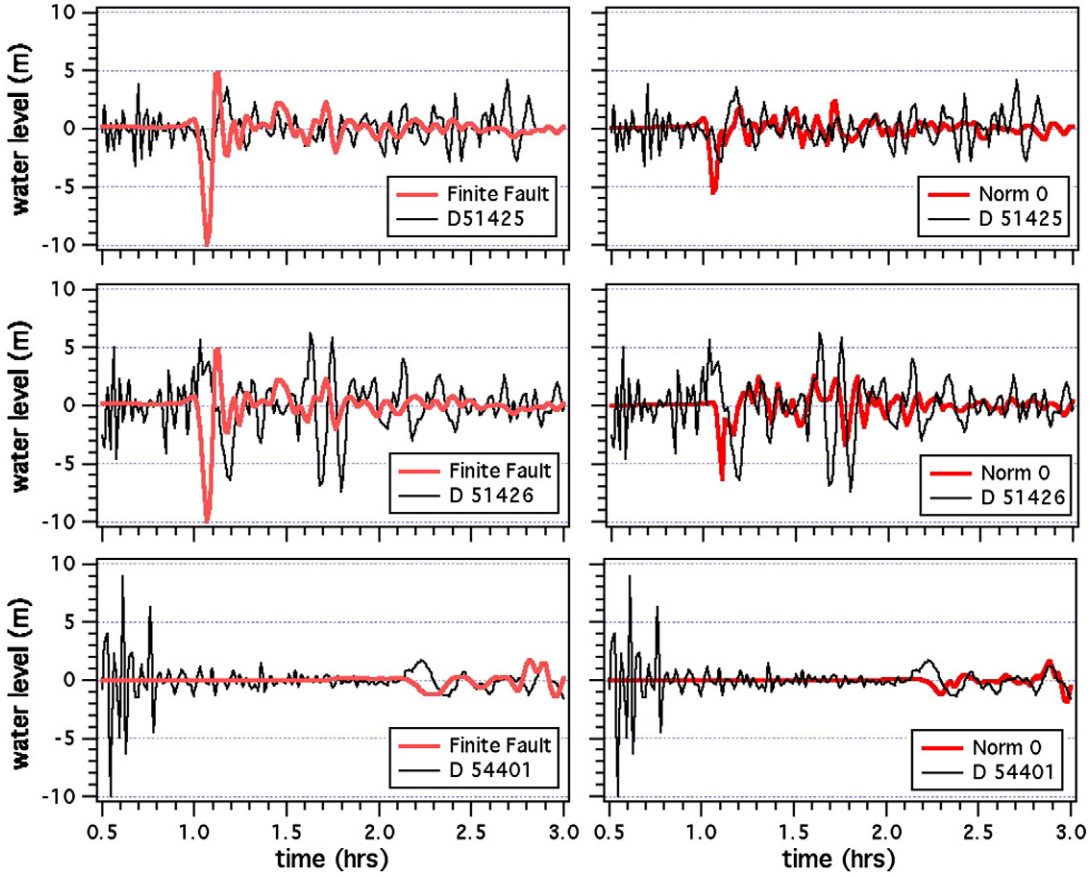

Fig. 12. Comparison between modeled (red) and measured water levels at three DART tsunameter locations for the Finite Fault and Norm 0 source models.

polarity relative to the DART data. It should be noted that these results are very similar to the results presented in Roeber et al. (2010).

6. Conclusions

Based on our modeling, a single normal fault source mechanism, with or without descriptions of the detailed slip distribution, is able to satisfactorily explain the tsunami behavior in Pago Pago Harbour. The addition of a megathrust source, as suggested by seismological and GPS data does not improve the model results there. Shifting the relative timing of the two sources offers some improvement, however these results are still not as good as the single, normal fault source. In the far-field, the megathrust source produces a very good fit to the observed initial wave signal on DART station 51426 and 54401 with a less good fit on station 51425. The normal fault sources alone do not provide a good fit to the observed data, except for the timing and magnitude of the initial drawdown seen on DART 51525. Combining the two time series does not significantly improve the fit between the modeled and measured data.

The 2009 South Pacific tsunami highlights yet again the extreme hazards from near source tsunamis where the earthquake is the 'official' warning. From the eyewitness accounts we infer that tsunami signage installed on Tutuila only months before the event helped save lives, and that misinformation and confusion regarding evacuation routes led to unnecessary casualties on Upolu and Niuatoputapu. We thus conclude that community-based education and awareness programs are essential in saving lives.

Author contributions

All authors participated in the Samoan archipelago tsunami field survey. H.M.F. and E.A.O. surveyed the tsunami in Tonga. J.C.B. conducted the numerical modeling.

Acknowledgements

This research was supported by the National Science Foundation NSF RAPID-award OCE-1000694.

References

Beavan, J., Wang, X., Holden, C., Wilson, K., Power, W., Prasetya, G., Bevis, M., Kautoke, R., 2010. Near-simultaneous great earthquakes at Tongan megathrust and outer rise in September 2009. Nature 466, 959–964. doi:10.1038/nature09292.

Fritz, H.M., Kalligeris, N., 2008. Ancestral heritage saves tribes during 1 April 2007 Solomon Islands tsunami. Geophys. Res. Lett. 35, L01607. doi:10.1029/2007GL031654.

Fritz, H.M., Borrero, J.C., Synolakis, C.E., Yoo, J., 2006. 2004 Indian Ocean tsunami flow velocity measurements from survivor videos. Geophys. Res. Lett. 33, L24605. doi:10.1029/2006GL026784.

Fritz, H.M., Kongko, W., Moore, A., McAdoo, B., Goff, J., Harbitz, C., Uslu, B., Kalligeris, N., Suteja, D., Kalsum, K., Titov, V., Gusman, A., Latief, H., Santoso, E., Sujoko, S., Djulkarnaen, D., Sunendar, H., Synolakis, C.E., 2007. Extreme runup from the 17 July 2006 Java tsunami. Geophys. Res. Lett. 34, L12602. doi:10.1029/2007GL029404.

Govers, R., Wortel, M.J.R., 2005. Lithosphere tearing at STEP faults: response to edges of subduction zones. Earth Plan. Sci. Lett. 236, 505–523.

Hayes, G., 2009. http://earthquake.usgs.gov/earthquakes/eqinthenews/2009/us2009mdbi/finite_fault.php.

Kirby, S.H., Hino, R., Geist, E.L., Wright, D.J., Okal, E.A., Wartman, J.M., 2009. Tectonic settings of great outer-rise/outer-trench-slope (OR/OTS) earthquakes in the instrumental record. Eos Trans. AGU 90, 52 Fall Meet. Suppl., Abstract U21D-06.

Lay, T., Ammon, C.J., Kanamori, H., Rivera, L., Koper, K.D., Hutko, A.R., 2010. The Samoa–Tonga great earthquake triggered doublet. Nature 466, 964–968. doi:10.1038/nature09214.

Li, X., Shao, G., Ji, C., 2009. Rupture process of $M_w = 8.1$ Samoa earthquake constrained by joint inverting teleseismic body, surface waves and local strong motion. Eos Trans. AGU 90, 52 Fall Meet. Suppl., Abstract U21D-03..

Liu, P.L.-F., Lynett, P., Fernando, J., Jaffe, B., Fritz, H., Higman, B., Morton, R., Goff, J., Synolakis, C., 2005. Observations by the International Tsunami Survey Team in Sri Lanka. Science 308 (5728), 1595.

Okal, E.A., Borrero, J.C., Synolakis, C.E., 2004. The earthquake and tsunami of 1865 November 17: evidence for far-field tsunami hazard from Tonga. Geophys. J. Int. 157, 164–174.

Okal, E.A., Fritz, H.M., Synolakis, C.E., Borrero, J.C., Weiss, R., Lynett, P.J., Titov, V.V., Foteinis, S., Jaffe, B.E., Liu, P.L.-F., Chan, I.-C., 2010. Field survey of the Samoa tsunami of 29 September 2009. Seismol. Res. Lett. 81, 577–591. doi:10.1785/gssrl.81.4.577.

Roeber, V., Yamazaki, Y., Cheung, K.F., 2010. Resonance and impact of the 2009 Samoa tsunami around Tutuila. AS. Geophys. Res. Lett. 37, L21604. doi:10.1029/2010GL044419.

Solov'ev, S.L., Go, Tch.N., Kim, Kh.S., 1986. Katalog tsunami v tikhom okeane, 1969–1982 gg. Akad. Nauk SSSR 164 pp., Moskva.

Synolakis, C.E., Okal, E.A., 2005. 1992–2002: perspective on a decade of post-tsunami surveys. In: Satake, K. (Ed.), Tsunamis: case studies and recent developments: Adv. Natur. Technol. Hazards, 23, pp. 1–30.

Tadepalli, S., Synolakis, C.E., 1994. The run-up of N-waves on sloping beaches. Proc. R. Soc. Lond. A Math. Phys. Sci. 445 (1923), 99–112.

Titov, V.V., Gonzalez, F., 1997. Implementation and Testing of the Method of Splitting Tsunami (MOST) Model. NOAA Technol. Memo. ERL PMEL-112.

Wall Street Journal, 2009. http://online.wsj.com/article/SB125086852452149513.html.

Yeh, H., Liu, P.L.-F., Briggs, M., Synolakis, C.E., 1994. Propagation and amplification of tsunamis at coastal boundaries. Nature 372 (24), 353–355.